ISBN: 978-3-95450-214-1 ISSN: 2673-5490 doi:10.18429/JACoW-IPAC2021-MOPAB352

# HIGH POWER TEST OF A DIELECTRIC DISK LOADED ACCELERATOR FOR A TWO BEAM WAKEFIELD ACCELERATOR*

B. Freemire†, C. Jing, S. Poddar, Euclid Beamlabs, 60440 Bolingbrook, USA
Y. Zhao, Euclid Techlabs, 60440 Bolingbrook, USA
M. Conde, D. S. Doran, G. Ha, W. Liu, M. Peng, J. G. Power, J. Shao, C. Whiteford, E. E. Wisniewski, Argonne National Laboratory, 60439 Lemont, USA

*Abstract*

As one of the candidate accelerating structures of the Argonne 500 MeV short pulse Two Beam Wakefield Acceleration Demonstrator, a single cell X-band dielectric disk loaded accelerator (DDA) has been designed, fabricated, and tested at high power at the Argonne Wakefield Accelerator. The DDA should provide a short pulse (~20 ns) high gradient (>300 MV/m) accelerator while maintaining a reasonable r/Q and high group velocity. This will allow a significantly larger RF-to-beam efficiency than is currently possible for conventional accelerating structures. A low loss barium titantate ceramic, $\epsilon_r = 50$, was selected, and a low temperature brazing alloy chosen to preserve the dielectric properties of the ceramic during brazing. High power testing produced breakdown at the triple junction, resulting from the braze joint design. No evidence of breakdown was observed on the iris of the disk, indicating that the maximum surface electric field on the dielectric was not reached. An improved braze joint has been designed and is in production, with high power testing to follow.

## INTRODUCTION

Two-beam acceleration (TBA) utilizes the wakefields excited by a high-charge drive beam traveling through one structure to power a second structure used to accelerate a low-charge main beam [1,2]. The Argonne Wakefield Accelerator (AWA) facility is pursuing short pulse TBA technology [3]. Recent evidence suggests that the RF breakdown rate is proportional to pulse length [4], and a ~20 ns pulse length has been chosen with the expectation of achieving an accelerating gradient of 270 MV/m.

Short RF pulses make it challenging to achieve a reasonable RF-to-main-beam efficiency. The combination of high group velocity, shunt impedance and quality factor is typically unattainable in conventional accelerating structures. For the proposed 3 TeV Argonne Flexible Linear Collider (AFLC), based on TBA, the baseline 26 GHz dielectric-loaded accelerator leads to an RF-to-main-beam efficiency of 27%, which is the bottleneck of the overall wall-plug efficiency [2,5].

A dielectric disk accelerator utilizing a high permittivity, low loss ceramic allows a 26 GHz DDA to simultaneously achieve a high group velocity, shunt impedance, and quality factor [6,7]. The RF-to-main-beam efficiency is estimated to be 39%, a 50% improvement over the baseline AFLC design. A prototype DDA was designed, fabricated, and tested at high power in an effort to demonstrate this short pulse, high gradient type of accelerating structure.

## X-BAND SINGLE CELL DDA DESIGN AND FABRICATION

A single cell X-band DDA structure was designed to be fed by the power extraction and transfer structure (PETS) at the AWA. The DDA prototype consisted of a single dielectric cell with two matching metallic cells, as shown in Fig. 1. The goals for this prototype were to determine a suitable brazing procedure for this ceramic, a barium titanate (BaTi), and measure the ceramic surface electric field breakdown threshold.

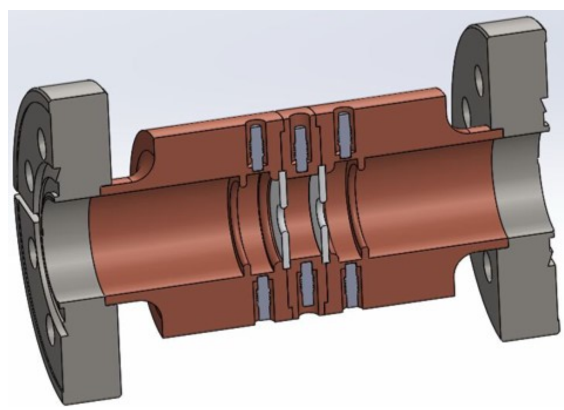

Figure 1: Cutaway view of the mechanical design of the DDA showing the dielectric cell and two matching metallic cells.

The measured dielectric constant and loss tangent of BaTi witness coupons as well as several simulated parameters of the DDA prototype are given in Table 1.

Two brazing methods were pursued. The first utilized an active brazing alloy (ABA) and brazing was performed at 835 °C in a vacuum furnace. This resulted in a significant increase in the loss tangent and minor change in the dielectric constant. A post-braze bake in air returned the loss tangent to 26% of the original value and slightly decreased the dielectric constant further. The second braze method utilized a BaTi disk metallized with silver in air then brazed with a gold-tin non-active alloy at 350 °C in vacuum. This method did not affect the dielectric properties of the ceramic and was chosen for fabrication of the DDA prototype.

* Work supported by DOE SBIR Grant DE-SC0019864 and DOE Office of Science Contract DE-AC02-06CH11357
† b.freemire@euclidtechlabs.com

ISBN: 978-3-95450-214-1 ISSN: 2673-5490 doi:10.18429/JACoW-IPAC2021-MOPAB352

Table 1: Simulated Parameters of the DDA Prototype

| Parameter | Value |
|---|---|
| Dielectric constant | 50.1 |
| Loss tangent | $8.0 \times 10^{-5}$ |
| Frequency | 11.7 GHz |
| Quality factor | 11,000 |
| Shunt impedance per unit length | 176 MΩ/m |
| Group velocity | 0.345 c |
| Phase advance | $2\pi/3$ |
| $E_{surface,max}/E_{acc}$ | 1.84 |
| $E_{surface,max}$ @ 500 MW | 245 MV/m |
| $E_{acc}$ @ 280 MW | 100 MV/m |

## HIGH POWER TEST RESULTS

The DDA prototype was tested using the PETS at the AWA, which is able to provide short (~10 ns) high power (up to 500 MW) RF pulses at 11.7 GHz [8,9]. During commissioning, the input power to the DDA was slowly increased. At low input power, the measured transmitted power through the DDA matched the simulated value well - Fig. 2.

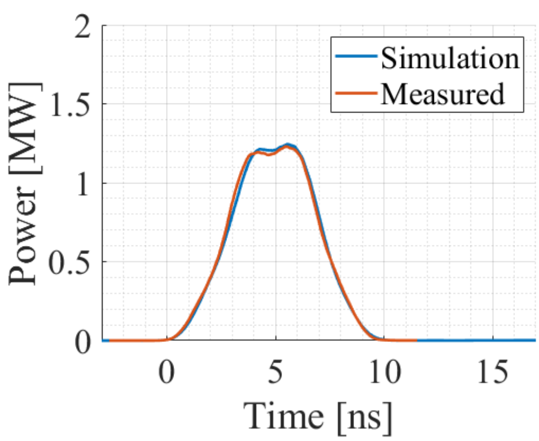


Figure 2: Measured (red) and simulated (blue) transmitted power through the DDA during low power operation.

Around 40 MW input power, light was visible around the circumference of the ceramic disks in the region of the braze joint - Fig. 3. The transmitted power was also less than expected - Fig. 4 - indicating a region of multipacting/loading. Conditioning was performed at this power level, which improved the transmitted power and light from the braze region.

At higher input power levels, significant loading and breakdown was observed, which could not be conditioned away. The high power test was concluded at an input power of 80 MW.

## POST MORTEM INSPECTION

After the high power test, the DDA prototype was wire EDM cut to inspect the ceramic surface. There was no

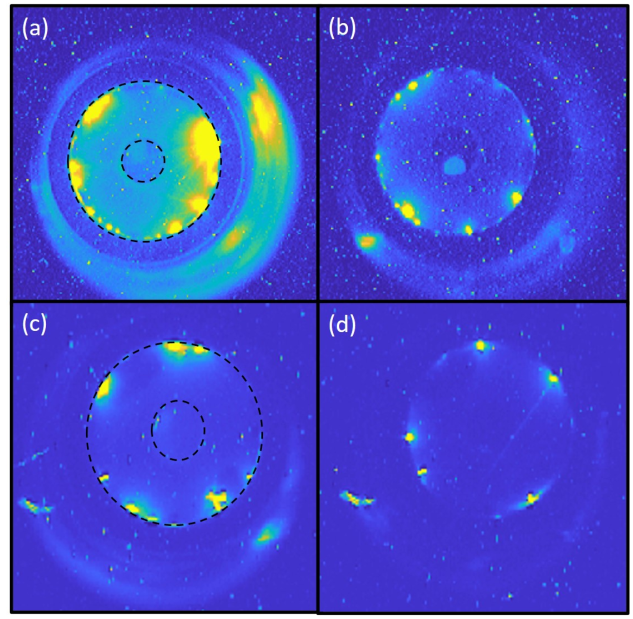


Figure 3: Snapshots of the face of the upstream (a & b) and downstream (c & d) disks, taken at the beginning (a & c) and end (b & d) of conditioning.The extents of the ceramic marked with dashed black lines on the left.

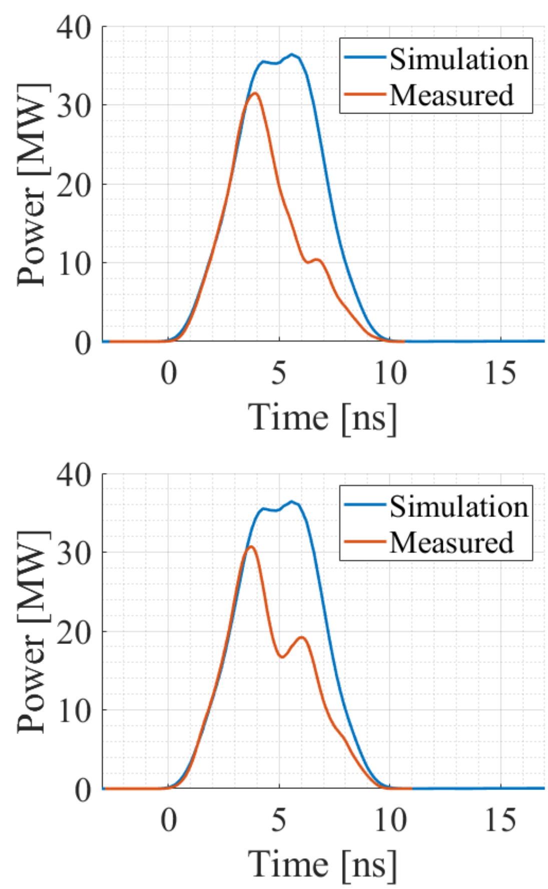


Figure 4: Measured (red) and simulated (blue) power at the output of the DDA before (top) and after (bottom) conditioning.

ISBN: 978-3-95450-214-1 ISSN: 2673-5490 doi:10.18429/JACoW-IPAC2021-MOPAB352

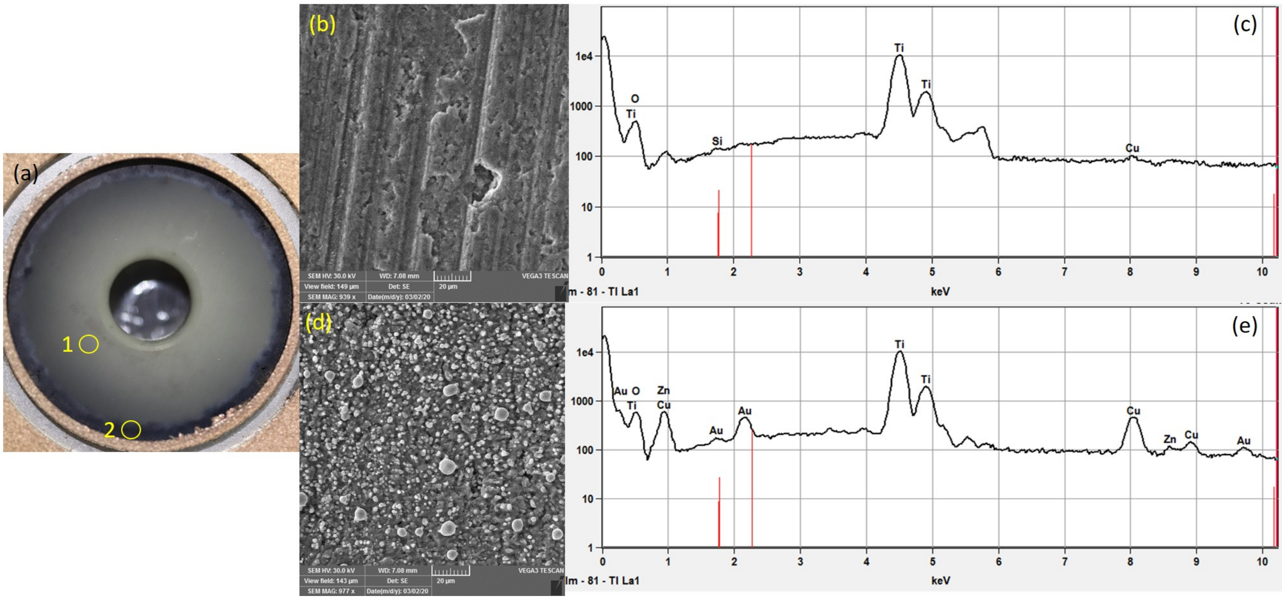


Figure 5: Photo of the interior face of one BaTi disk (a). SEM and EDX data were collected at locations indicated by the numbered circles: 1 corresponds to (b & c), and 2 to (d & e).

evidence of breakdown on the ceramic iris, however the ceramic in the region of the braze joint was severely damaged. Figure 5 shows a photo of the interior face of one BaTi disk, as well as SEM and EDX data collected near the iris and braze joint. The ceramic face near the iris shows only machining marks and has minimal contamination. The ceramic face near the braze joint is highly textured and contains gold and copper deposited likely as a result of breakdown.

Increasing the mesh density in the region of the triple junction (braze joint) in the simulation model revealed significantly larger field enhancement than originally thought - Fig. 6. The electric field at the braze joint was nearly as large as on the ceramic iris, and was the cause of multipacting and breakdown.

## FUTURE DDA PROTOTYPE DESIGN

To avoid field enhancement at the triple junction and issues involved with brazing, a clamped DDA structure has been designed and is being fabricated. Elliptic rounding added to the copper and ceramic ensures the peak surface electric field is on the ceramic iris.

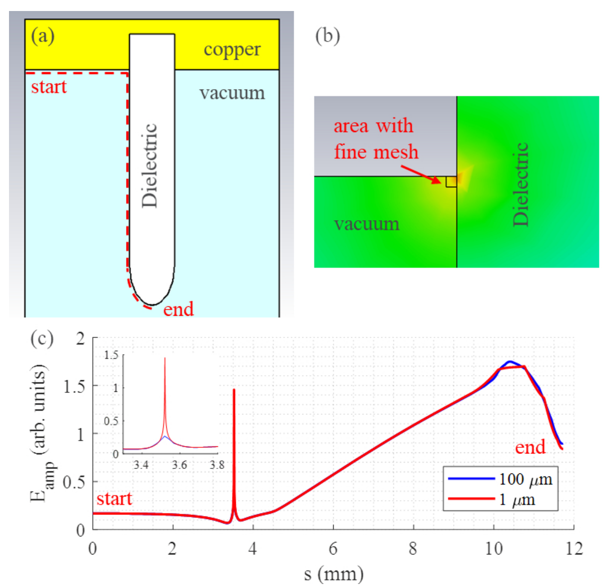


Figure 6: Increased mesh density at the triple junction (b) revealed field enhancement at the braze joint (a & c) comparable to that on the ceramic iris.

## REFERENCES


[1] B. Cros and P. Muggli, “Towards a Proposal for an Advanced Linear Collider Report on the Advanced and Novel Accelerators for High Energy Physics Roadmap Workshop”, CERN, Geneva, Apr. 2017. http://cds.cern.ch/record/2298632

[2] C. Jing, “Dielectric Wakefield Accelerators”, *Rev. Accel. Sci. Technol.*, vol. 09, p. 127, 2016. doi:10.1142/S1793626816300061

[3] M. Conde *et al.*, “Research program and recent results at the Argonne Wakefield Accelerator facility (AWA)”, in *Proc. 8th International Particle Accelerator Conference (IPAC’17)*, Copenhagen, Denmark, 2017, pp. 2885-2887. doi:10.18429/JACoW-IPAC2017-WEPAB132

[4] A. Grudiev, S. Calatroni, and W. Wuensch, “New local field quantity describing the high gradient limit of accelerating structures”, *Phys. Rev. ST Accel. Beams*, vol. 12, no. 10, p. 102001, 2009. doi:10.1103/physrevstab.12.102001

[5] W. Gai, J. G. Power, and C. Jing, “Short-pulse dielectric two-beam acceleration”, *J. of Plasma Phys.*, vol. 78, no. 4, pp. 339–345, Feb. 2012. doi:10.1017/s0022377812000037

ISBN: 978-3-95450-214-1 ISSN: 2673-5490 doi:10.18429/JACoW-IPAC2021-MOPAB352

[6] J. Shao, M. Conde, C. Jing, D. Doran, and J. Power, "Study of a dielectric disk structure for short pulse two-beam acceleration", in *Proc. 9th International Particle Accelerator Conference*, Vancouver, BC, Canada, 2018, pp 1539-1541. doi:10.18429/JACoW-IPAC2018-TUPML005

[7] C. Jing, J. Shao, J. Power, M. Conde, and S. Doran, "Dielectric Disk Accelerator for High Gradient Short Pulse Two-Beam Wakefield Acceleration", in *2018 IEEE Advanced Accelerator Concepts Workshop (AAC)*, pp. 1–5, 2018. doi:10.1109/aac.2018.8659397

[8] J. Shi *et al.*, "Development Of An X-Band Metallic Power Extractor For The Argonne Wakefield Accelerator", in *Proc. 4th International Particle Accelerator Conference (IPAC'13)*, Shanghai, China, May 2013, paper WEPFI031, pp. 2771-2773.

[9] M. Peng *et al.*, "Generation of high power short rf pulses using an X-band metallic power extractor driven by high charge multi-bunch train", in *Proc. of the 10th International Particle Accelerator Conference (IPAC'19)*, Melbourne, Australia, May 2019, pp. 734-737. doi:10.18429/JACoW-IPAC2019-MOPRB069